AN EXACT SOLUTION FOR DROPLET VAPORIZATION WITH VARIABLE TRANSPORT COEFFICIENT

Daniela de Oliveira Maionchi
Instituto de Física, Universidade Federal de Mato Grosso, 78060-900, Cuiabá, MT, Brazil
dmaionchi@fisica.ufmt.br

Fernando Fachini Filho
Grupo de Mecânica de Fluidos Reativos, Laboratório de Combustão e Propulsão, Instituto Nacional de Pesquisas Espaciais, 12630-000, Cachoeira Paulista, SP, Brazil
fachini@lcp.inpe.br

Abstract. *This work presents an analytical solution for the vaporization rate of an isolated droplet in quiescent environment by including a temperature dependence in the gas phase transport properties. The transport properties are well described by the square root of temperature. The droplet heating and vaporization are described analytically considering this dependence and the results are compared with that obtained with the classical model (constant transport properties). They show that the droplet heating time is longer in the case including temperature dependence in the properties and, consequently, the vaporization rate is smaller. Both models coincide in case of droplet cooling.*

Keywords: *droplet vaporization, variable transport coefficient, uniform droplet temperature.*

1. INTRODUCTION

Spray combustion is mainly controlled by fuel atomization. It breaks liquid fuels in a huge number of droplets, whose distribution is only described statistically. By producing a high number of droplets, the contact area between gas and liquid phases is increased, permitting larger heat fluxes to the fuel droplets and, consequently, an expressive fuel vaporization rate. Besides breaking the liquid fuel, atomization process spreads it in form of droplets inside the combustion chamber, leading to the specification of the fuel concentration along this chamber and its mixture with the oxidant. Based on this picture, the analysis of heating, vaporization and combustion problems of isolated droplets are fundamental for the comprehension of more complex systems, what is reflected in a large number of articles involving those issues (Faeth, 1977; Law, 1982; Sirignano, 1983; Dwyer, 1989; Chen *et al.*, 1996; Chiu, 2000; Sazhin, 2006; Birouk and Gakalp, 2006).

In order to develop a realistic running time numerical code for simulating spray combustion, analytical and low numerical cost models are mandatory to describe heating and vaporization of isolated droplet (Williams, 1985). Two simplified models are considered in literature: uniform temperature inside the droplet and temporal-spatial temperature determined by the conduction limit (Gutheil, 1993; Eropoulos, 1984). In both models, the transport coefficient is constant for the gas phase surrounding the droplet and the droplet is at a quiescent environment, permitting an analytical solution for the vaporization rate to be found (Williams, 1985). Based on these results, heating and vaporization rates for droplets with relative velocity with gas phase are calculated (Birouk and Gakalp, 2006). Therefore, an improvement in the model for heating and vaporization rates considering a temperature dependence on the transport coefficients for the gas phase will provide more reliable results.

In section 2, the mathematical formulation for a droplet vaporization model with variable transport coefficient in the gaseous phase is developed. In section 3, results are presented and compared with the simple model normally considered in literature. Finally, in section 4 conclusions are stated and applications of the model in future works are presented.

2. MATHEMATICAL FORMULATION

The conditions addressed in this work permit considering the gas phase close to the droplet in a quasi steady regime. The formulation follows that of a quasi-steady droplet combustion problem (Fachini, 1999).

It is assumed that the density ρ_l, the specific heat c_l and the thermal conductivity k_l of the liquid phase are constants. Far from the droplet, the gas has constant properties, more specifically, density ρ_∞, thermal conductivity $k_{g\infty}$ and pressure specific heat c_p. The gas temperature far from the droplet is also held constant at T_∞. However, for the gas phase, the transport coefficients (thermal conductivity k_g and fuel diffusion coefficient D_F) depend only on temperature according to $k_g/k_{g\infty} = D_F/D_{F\infty} = (T/T_\infty)^n = \theta^n$. The normalized fuel mass fraction is identified by $Y_F \equiv y_F$.

The radial coordinate r relative to the initial droplet radius $\bar{a}_0$ and the dimensionless droplet radius a are defined as $x = r/\bar{a}_0$ and $a = \bar{a}/\bar{a}_0$, respectively. The description of the liquid phase is given by following mass and energy

dimensionless conservation equations

$$\frac{da^3}{d\tau} = -3\lambda,$$
(1)

$$\frac{\partial \theta}{\partial \tau} = \frac{\alpha_l}{x^2} \frac{\partial}{\partial x} \left(x^2 \frac{\partial \theta}{\partial x} \right),$$
(2)

valid for $x < a(\tau)$, in which $\tau \equiv t/t_c$ is the dimensionless time according to the order of magnitude of the droplet lifetime $t_c \equiv (\rho_\infty c_{\bar{p}} \bar{a}_0^2 / k_{g\infty})(\rho_l/\rho_\infty)$, $\lambda \equiv c_p \dot{m}/(4\pi \bar{a}_0 k_{g\infty})$ is the vaporization rate and $\alpha_l \equiv k_l c_p/(k_g c_l)$. The quantity $\dot{m}$ describes the dimensional vaporization rate.

The set of mass, species and energy conservation equations describing the processes in the gas phase $[x > a(\tau)]$ is given by

$$\varepsilon \frac{\partial \varrho}{\partial \tau} + \frac{1}{x^2} \frac{\partial}{\partial x}(x^2 \varrho v) = 0,$$
(3)

$$\varepsilon \frac{\partial}{\partial \tau}(\varrho Y_F) + \frac{1}{x^2} \frac{\partial}{\partial x}(x^2 \varrho v Y_F) = \frac{1}{x^2} \frac{\partial}{\partial x} \left(\frac{x^2 \theta^n}{Le_F} \frac{\partial Y_F}{\partial x} \right),$$
(4)

$$\varepsilon \frac{\partial}{\partial \tau}(\varrho \theta) + \frac{1}{x^2} \frac{\partial}{\partial x}(x^2 \varrho v \theta) = \frac{1}{x^2} \frac{\partial}{\partial x} \left(x^2 \theta^n \frac{\partial \theta}{\partial x} \right),$$
(5)

in which the density $\varrho \equiv \rho/\rho_\infty$ is measured in terms of ambient atmosphere density, the fuel Lewis number is $Le_F \equiv k_{g\infty}/(\rho_\infty c_p D_{F\infty})$ and the parameter $\varepsilon = \rho_\infty/\rho_l$ measures the thermal inertia of the gas phase in terms of that of the liquid phase. It is worth noting that the diffusion terms in Eqs.(4) and (5) contain a temperature dependence in the form θ^n. For $0 \leq n \leq 1$, the higher its value the slower is the heat transfer.

For the conditions addressed in this work $\varepsilon \ll 1$, which justifies the quasi-steady behavior for the gas phase.

The initial conditions for Eqs.(1) and (2) are

$$a = 1, \quad \theta(x < a) = \theta_0 \qquad \text{for } \tau = 0.$$
(6)

It is also considered that the fuel molecular weight equals that of the ambient gases mixture. At the liquid-gas interface, the vapor and liquid are assumed in equilibrium, so that Clausius-Clapeyron expression

$$Y_{Fs} = \exp[\gamma(1 - \theta_B/\theta_s)],$$
(7)

in which $\gamma = L/RT_B$, can be used to relate the temperature θ_s to the fuel mass fraction Y_{Fs} at the droplet surface. The boundary conditions necessary to solve the problem are

$$\left. \frac{\partial \theta}{\partial x} \right|_{x=0} = 0, \quad \left. a^2 \theta^n \frac{\partial \theta}{\partial x} \right|_{x=a^+} = \lambda l + K a^2 \left. \frac{\partial \theta}{\partial x} \right|_{x=a^-}, \quad \left. \frac{a^2 \theta^n}{Le_F} \frac{\partial Y_F}{\partial x} \right|_{x=a^+} = -\lambda(1 - Y_{Fs}),$$

$$\theta(x \to \infty) = \theta_\infty = 1, \quad Y_F(x \to \infty) = Y_{F\infty},$$
(8)

in which $l \equiv L/c_p T_\infty$ is the dimensionless latent heat and $K \equiv k_l/k_{g\infty}$ is the ratio of thermal conductivities of the droplet and ambient gaseous phase.

The quasi-steady behavior for the gas phase leads allows the integration of Eqs.(3) to (5), simplifying them to

$$x^2 \varrho v = \lambda,$$
(9)

$$\frac{x^2 \theta^n}{Le_F} \frac{\partial Y_F}{\partial x} = \lambda(Y_F - C_1),$$
(10)

$$x^2 \theta^n \frac{\partial \theta}{\partial x} = \lambda(\theta + C_2),$$
(11)

in which C_1 and C_2 are constants of integration. Applying boundary condition (8) for Y_{Fs} at droplet surface, C_1 must equal one. Eqs.(10) and (11) can be combined, leading to

$$\frac{(\theta + C_2)}{Le_F} \frac{\partial Y_F}{\partial \theta} = Y_F - 1.$$
(12)

Integrating it and applying the ambient atmosphere condition, the relation $\theta = \theta(Y_F)$ is found

$$\theta(Y_F) = -C_2 + (\theta_\infty + C_2) \left(\frac{1 - Y_F}{1 - Y_{F\infty}} \right)^{1/Le_F}.$$
(13)

By imposing the boundary condition at the droplet surface, the constant of integration C_2 is determined to be

$$C_2 = -\theta_s \left[1 - \frac{\theta_\infty}{\theta_s} \left(\frac{1 - Y_{Fs}}{1 - Y_{F\infty}} \right)^{1/Le_F} \right] \Big/ \left[1 - \left(\frac{1 - Y_{Fs}}{1 - Y_{F\infty}} \right)^{1/Le_F} \right]. \tag{14}$$

A qualitative analyses of Equations (11) and (14) shows that λC_2, which represents the conservation of local thermal energy and heat flux, describes a relation between conduction and convection. In case of droplet heating, the conduction term is positive, which means that heat is transferred to the droplet, then $C_2 > 0$; in case of droplet cooling, this term is negative, hence $C_2 < 0$. It is worth noting that C_2 does not depend on the exponent n.

The temperature profile can be obtained by integrating Eq.(11), which leads to

$$\int_{\theta_s}^{\theta} \frac{\theta^n}{\theta + C_2} d\theta = \lambda \left(\frac{1}{a} - \frac{1}{x} \right). \tag{15}$$

Once the energy conservation problem in the gas phase is solved, $\theta = \theta(x)$ and C_2 are specified and it is possible to integrate Eq.(10) leading to,

$$Le_F \lambda \int_a^x \frac{dx}{x^2 \theta^n(x)} = ln \left(\frac{1 - Y_F}{1 - Y_{Fs}} \right). \tag{16}$$

The droplet vaporization rate can be calculated from Equations (15) or (16) by imposing the ambient atmosphere boundary condition, that is

$$\lambda = \frac{1}{Le_F} ln \left(\frac{1 - Y_{F\infty}}{1 - Y_{Fs}} \right) \left(\int_a^\infty \frac{dx}{x^2 \theta^n(x)} \right)^{-1} = a \int_{\theta_s}^{\theta_\infty} \frac{\theta^n}{\theta + C_2} d\theta. \tag{17}$$

An analysis is performed for $n = 0$ and $1/2$. The description of droplet vaporization considering the solution for $n = 0$ is usual in literature and can be easily provided by Equations (15) and (17), leading to the following temperature and fuel mass fraction profiles

$$\theta(x) = -C_2 + (\theta_s + C_2) \exp \left[\lambda \left(\frac{1}{a} - \frac{1}{x} \right) \right], \tag{18}$$

$$Y_F(x) = 1 + (Y_{Fs} - 1) \exp \left[\lambda Le_F \left(\frac{1}{a} - \frac{1}{x} \right) \right]. \tag{19}$$

For this case, the vaporization rate $\beta \equiv \lambda/a$ obtained from Eq.(18) gives

$$\beta = \ln \left(\frac{1 - Y_{F\infty}}{1 - Y_{Fs}} \right)^{1/Le_F} = \ln \left(\frac{\theta_\infty + C_2}{\theta_s + C_2} \right). \tag{20}$$

This expression agrees with the the expression obtained in Eq.(14) for the constant C_2.

The integration Eq.(15) for $n = 1/2$ corresponds to a more realistic condition. Two cases must be considered in this situation: $C_2 > 0$ and $C_2 < 0$. Defining $\Theta \equiv \sqrt{\theta/|C_2|}$, the solution of this equation is given by

$$\frac{1}{2\sqrt{|C_2|}} \left[-\frac{\lambda}{x} + \frac{\lambda}{a} \right] = \Theta - \Theta_s - \begin{cases} \arctan \Theta - \arctan \Theta_s & \text{for } C_2 > 0, \\ \text{arctanh} \Theta - \text{arctanh} \Theta_s & \text{for } C_2 < 0. \end{cases} \tag{21}$$

The expression for β in this case can be evaluated by applying the ambient boundary condition in Eq.(21), giving

$$\frac{\beta}{2\sqrt{|C_2|}} = \Theta_\infty - \Theta_s - \begin{cases} \arctan \Theta_\infty - \arctan \Theta_s & \text{for } C_2 > 0, \\ \text{arctanh} \Theta_\infty - \text{arctanh} \Theta_s & \text{for } C_2 < 0. \end{cases} \tag{22}$$

In the limit of α_l large in Eq.(2), the temperature profile inside the droplet changes slightly with position, explaining the approximation $\theta(\tau, x) \sim \theta(\tau)$. With this property, this equation can be integrated over the range $0 \leq x \leq a$, which leads to

$$\frac{a^3}{3} \frac{d\theta_s}{d\tau} = \alpha_l a^2 \frac{\partial \theta}{\partial x} \Big|_{x=a^-}. \tag{23}$$

Taking Eqs.(11) into the boundary condition (7) at the droplet surface, an equation for describing droplet temperature evolution is found according to

$$Ca^3 \frac{d\theta_s}{d\tau} = -\lambda l + \lambda(\theta_s - C_2) = \lambda(\theta_s - l - C_2), \tag{24}$$

in which $C \equiv c_l/3c_p$. Therefore, the integration of Eq.(24) occurs simultaneously with integration of Eq.(1), solving at each time step Eqs.(14) and (20) or (22), for $n = 0$ or $1/2$, respectively.

3. RESULTS AND DISCUSSION

The simulations were performed for $n = 0$ and $1/2$. After a heating (or cooling) time the temperature does not change and this final state is defined as equilibrium because there is balance between the conduction heat from the gas phase to the liquid phase and the heat lost through vaporization. For cases of droplet cooling, the models considering $n = 0$ and $1/2$ produce the same results: the surface temperature and mass fraction present the same behavior for both cases, reaching its equilibrium state, characterized by the values $[\theta_S]_{eq}$ and $[Y_{Fs}]_{eq}$, respectively. Unlike this case, the models present different results for droplet heating. Besides that, heat will be absorbed or released by the droplet, depending if its initial surface temperature is lower or higher than the equilibrium values. It can be advanced that the more realistic model ($n = 1/2$) presents a lower vaporization rate than that with $n = 0$ and longer heating time. Also, both models provide the same equilibrium state.
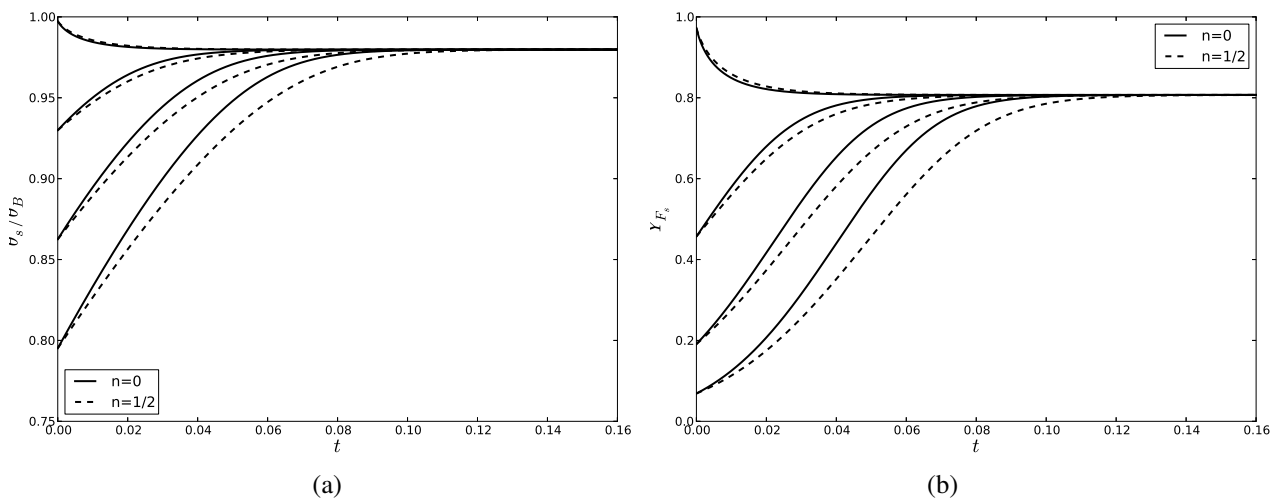

Figure 1: (a) Temperature and (b) fuel mass fraction profiles at the surface for $T_\infty = 800K$ and initial surface temperature 295, 320, 345 and 370 K.

Following the time evolution of the droplet surface temperature and the respective mass fraction, they increase slower for $n = 1/2$; hence, the equilibrium state is reached later, as depicted in Fig. 1. The reason for that is related to the heat flux from the gas phase to the liquid phase, which is smaller for $n = 1/2$ because $\theta_s^{1/2} < 1$ in the thermal conductivity (with $\theta_s < 1$).

From Fig. 1 it is possible to see that for all situations the droplet surface tends to an equilibrium state described by $[\theta_s]_{eq}$. The dependence of this value on the ambient temperature is plotted in Fig. 2. For both $n = 0$ and $1/2$ the curve obtained is the same, indicating an independence on the conductivity model.
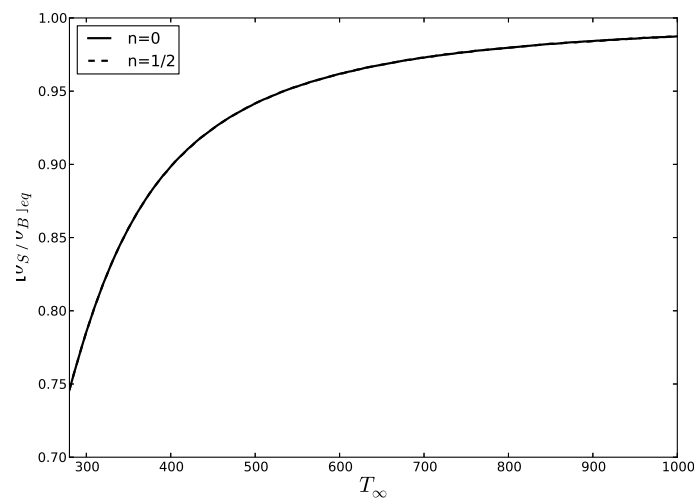

Figure 2: Equilibrium surface temperature as a function of T_∞

Although the equilibrium surface temperature independs on the ambient temperature and thermal conductivity model, it is interesting to analyse how the vaporization rate varies during vaporization for both cases. The evolution of both λ
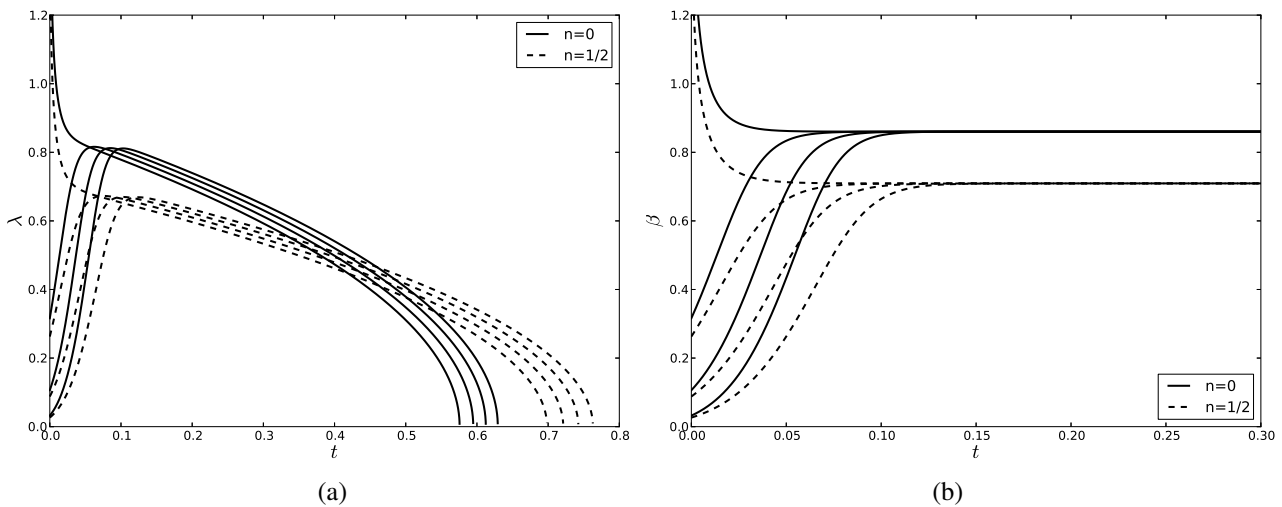
(a)   (b)

Figure 3: (a) λ and (b) β profiles for $T_\infty = 800K$ and initial surface temperature 295, 320, 345 and 370 K.

and β are presented in Fig. 3. From this figure, the classical results are recuperated, i.e. β is constant after the heating (cooling) period.

The square of droplet radius decrease linearly in time, as can be seen in Fig.4 a. Although the heating time depends on the droplet initial temperature, which defines the droplet lifetime, the slope of the curve is independent of this temperature for a given value of n. It happens because the vaporization rate measured from the slope reaches a constant value that is determined by the atmospheric ambient via the heat flux to the droplet.

From Fig. 1, one can see that the heating time for the droplet to reach the equilibrium surface temperature depends on the value of n. The heating times for the droplet to reach 0.99 of the equilibrium surface temperature for $n = 0$ and $1/2$ are defined as t_0 and $t_{1/2}$, respectively. Figure 4 b shows the relative difference $(t_{1/2} - t_0)/t_0$ as a function of ambient temperature. The initial droplet surface temperature practically does not influence the heating time. This plot summarizes the importance of substituting the previous model with $n = 0$ by the one presented in this work for $n = 1/2$, as almost 30% of relative vaporization time difference can be observed for high ambient temperature.
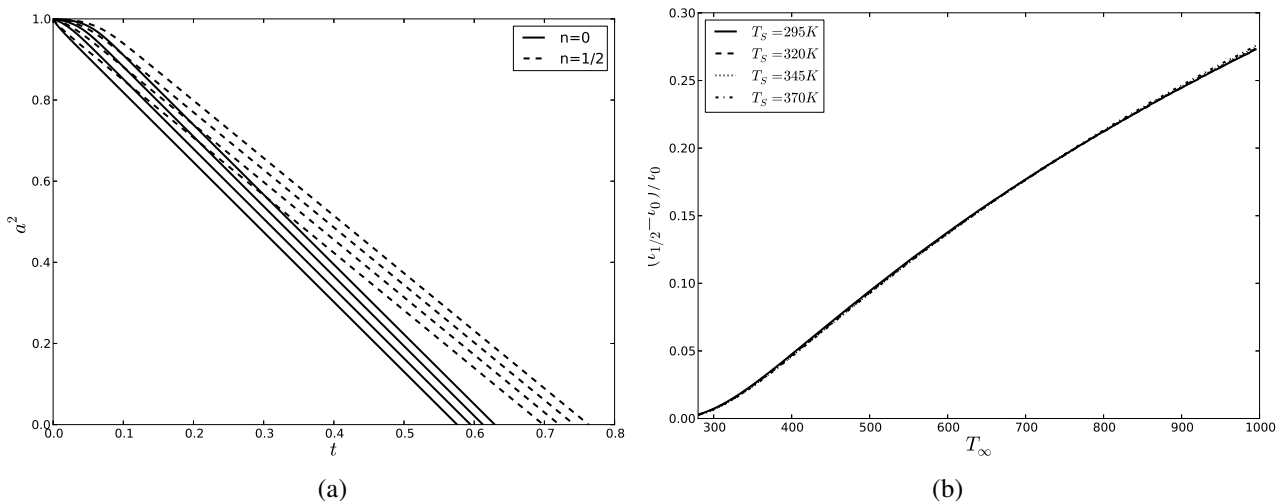

(a)   (b)

Figure 4: (a) Droplet radius evolution for $T_\infty = 800K$ and initial surface temperature 295, 320, 345 and 370 K. (b) Relative time difference adopting $n = 0$ or $n = 1/2$ in the model for initial surface temperature 295, 320, 345 and 370 K.

3.1 CONCLUSION

In this work a model for droplet vaporization with a more realistic expression for the gas phase thermal conductivity was presented. The model is able to simulate a heating time about $10 - 30\%$ higher than the classical model ($n = 0$) for the droplet heating problem. In case of droplet cooling, the model with $n = 1/2$ presents no important improvement on that one with $n = 0$. The droplet surface temperature and the fuel mass fraction reach an equilibrium state which independs on the model.

These results provide an analytical solution that can be included in spray combustion models for droplet vaporization

(Maionchi and Fachini, 2013). Besides that, a constant was found in terms of the surface and ambient temperature and fuel mass fraction, which is independent of the value n considered in the diffusion term on both species and energy conservation equations.

4. ACKNOWLEDGEMENTS

5. REFERENCES

Birouk, M. and Gakalp, I., 2006. "Current status of droplet evaporation in turbulent flows". *Progress in Energy and Combustion Science*, Vol. 32, pp. 408–423.

Chen, G., Mazumder, M., Chang, R., Swindal, J. and Acker, W., 1996. "Laser diagnostics for droplet characterization: Application of morphology dependent resonances". *Progress in Energy and Combustion Science*, Vol. 22, pp. 163–188.

Chiu, H., 2000. "Advances and challenges in droplet and spray combustion. i. toward a unified theory of droplet aerothermochemistry- review article". *Progress in Energy and Combustion Science*, Vol. 26, pp. 381–416.

Dwyer, H., 1989. "Calculations of droplet dynamics in high temperature environments". *Progress in Energy and Combustion Science*, Vol. 15, pp. 131–158.

Eropoulos, C., 1984. "Flame propagation in aerosols of fuel droplets, fuel vapor and air". *Comb. Sci. Technol.*, Vol. 40, pp. 217–232.

Fachini, F., 1999. "An analytical solution for the quasi-steady droplet combustion". *Combustion and Flame*, Vol. 116, pp. 302–306.

Faeth, G., 1977. "Current status of droplet and liquid combustion". *Progress in Energy and Combustion Science*, Vol. 3, pp. 191–224.

Gutheil, E., 1993. "Numerical investigation of the ignition of dilute fuels sprays including detailed chemistry". *Combustion and Flame*, Vol. 93, pp. 239–254.

Law, C., 1982. "Recent advances in droplet vaporization and combustion". *Progress in Energy and Combustion Science*, Vol. 8, pp. 171–201.

Maionchi, D. and Fachini, F., 2013. "A simple spray-flamelet model: Influence of ambient temperature and fuel concentration, vaporization source and fuel injection position". *Combustion Theory and Modelling (online)*.

Sazhin, S., 2006. "Advanced models of fuel droplet heating and evaporation". *Progress in Energy and Combustion Science*, Vol. 32, pp. 162–214.

Sirignano, W., 1983. "Fuel droplet vaporization and spray combustion theory". *Progress in Energy and Combustion Science*, Vol. 9, pp. 291–322.

Williams, F., 1985. *Combustion Theory*. The Benjamin/Cummings Publishing Company.

6. RESPONSIBILITY NOTICE

The authors are the only responsible for the printed material included in this paper.